International Nano Letters
a SpringerOpen Journal

ORIGINAL ARTICLE Open Access

Hydrothermal synthesis, characterization, and investigation of optical properties of Sb^{3+}-doped lithium silicates nanoparticles

Abdolali Alemi[1], Shahin Khademinia[1*], Mahboubeh Dolatyari[2] and Akbar Bakhtiari[1]

Abstract

The hydrothermal synthesis and optical properties of undoped and Sb^{3+}-doped lithium metasilicate and lithium disilicate nanomaterials were investigated. The microstructures and morphologies of the synthesized $Li_{2-2x}Sb_{2x}SiO_3$ and $Li_{2-2x}Sb_{2x}Si_2O_5$ nanoparticles were studied with powder X-ray diffraction and scanning electron microscopy techniques, respectively. The synthesized undoped and doped lithium metasilicate and lithium disilicate nanomaterials, respectively, are isostructural with the standard bulk Li_2SiO_3 (space group $Cmc2_1$) and $Li_2Si_2O_5$ (space group Ccc2) materials. The electronic absorption and photoluminescence spectra of the synthesized materials are studied. The measured optical properties show dependence on the dopant amounts in the structure.

Keywords: Nanoparticle, Lithium silicate, Doped material, Antimony, Hydrothermal

Background

Lithium ceramics are of research interest because of their technological applications. Among these ceramics, lithium silicates have been investigated as breeder materials for nuclear fusion reactors and as carbon dioxide absorbents in addition to other more well-known applications such as in thermal expansion of glass ceramics used in ceramic hobs [1-6]. Since the tetrahedral silicate ion (SiO_4^{2-}) provides good mechanical resistance and stability, lithium metasilicate, and lithium disilicate are used as pyroelectric materials in optical waveguide devices [7-12].

Previously, some research groups have reported the synthesis of lithium silicate doped with La^{3+}, Sm^{3+}, Gd^{3+}, Ho^{3+}, Dy^{3+} [13-16], Nd^{3+} [17], Eu^{3+}, and Tb^{3+} [18] ions. Also, Cr^{4+}-doped [19], Al^{3+}-doped [20], and Na^{+}-doped [21] lithium silicates have been synthesized. Moreover, Rodriguez et al have reported the synthesis of Cr^{3+}-and Tm^{3+}-doped alkaline silicate glasses [22]. On the other hand, Cu^{2+}-doped [23] and V^{5+}-doped [24] lithium disilicate glasses have been reported previously. However, to our best knowledge, no work has been devoted to antimony-doped lithium silicates. Catalytic activity [25], photo-induced superhydrophilicity [26], and optoelectronic properties [27] are observed in Sb^{3+}-doped materials. Sb^{3+}-doped semiconductors exhibit increased electrical conductivity compared to the undoped materials [28,29]. The doping of Sb^{3+} also causes a p-type connection and pins the Fermi level in metal-semiconductor interface [30,31].

In this context, we sought to reexamine the chemistry of lithium silicates. Herein, we report the hydrothermal synthesis of the Sb^{3+}-doped lithium metasilicate ($Li_{2-2x}Sb_{2x}SiO_3$) and lithium disilicate ($Li_{2-2x}Sb_{2x}Si_2O_5$) nanoparticles. The effect of the dopant concentration on the morphology of the synthesized materials is investigated. Moreover, the optical properties of the synthesized $Li_{2-2x}Sb_{2x}SiO_3$ and $Li_{2-2x}Sb_{2x}Si_2O_5$ nanomaterials are studied.

Methods

The phase identifications were performed on a powder X-ray diffractometer Siemens D5000 (Siemens AG, Munich, Germany) using Cu-K_α radiation. The morphology of the obtained materials was examined by a Philips XL30 scanning electron microscope (Royal Philips Electronics, Amsterdam, The Netherlands). Absorption and photoluminescence spectra were recorded on a Analytik Jena Specord 40 (Analytik Jena AG Analytical

* Correspondence: shahinkhademinia@gmail.com
[1]Department of Inorganic Chemistry, Faculty of Chemistry, University of Tabriz, Tabriz, Iran
Full list of author information is available at the end of the article

Instrumentation, Jena, Germany) and a Perkin Elmer LF-5 spectrometer (PerkinElmer Inc., Waltham, MA, USA), respectively.

All the reagents used in the experiments were of analytical grade and used as received without further purification. The $Li_{2-2x}Sb_{2x}SiO_3$ and $Li_{2-2x}Sb_{2x}Si_2O_5$ nanomaterials are synthesized in a one-step hydrothermal process.

Synthesis of lithium metasilicate

$LiNO_3$ (2 mmol) was added to a solution of silicic acid (4 mmol) in 30 mL of hot 0.01 M aqueous solution of NaOH while stirring. The resultant solution was stirred for further 15 min and then diluted to 60 mL. The obtained mixture was transferred to a 100-mL Teflon-lined stainless steel autoclave and heated for 48, 72, or 96 h at 180°C. The resulting nanomaterials of Li_2SiO_3 were filtered and dried at 110°C.

Synthesis of lithium disilicate

The preparation of $Li_2Si_2O_5$ was similar to that of Li_2SiO_3, except that $LiNO_3$ (2 mmol) and silicic acid (6 mmol) were used. The obtained mixture was transferred to a 100-mL Teflon-lined stainless steel autoclave and heated for 48, 72, 96, or 120 h at 180°C. The resulting nanomaterials of compound $Li_2Si_2O_5$ were filtered and dried at 110°C.

Synthesis of Sb^{3+}-doped lithium metasilicate ($x = 0.01$, 0.0125, and 0.015)

Appropriate molar amounts of $LiNO_3$ (7.9, 5.87, or 5.90 mmol), $SiO_2.H_2O$ (15.88, 11.82, or 11.91 mmol, respectively), and Sb_2O_3 (0.0387, 0.0398, or 0.0449 mmol, respectively) were dissolved in 60 mL of hot NaOH solution (0.53, 0.40, or 0.40 M, respectively) under magnetic stirring at 80°C. The resultant solution was transferred into a 100-mL Teflon-lined stainless steel autoclave. The autoclave was sealed and maintained at 180°C for 48 h then allowed to cool naturally to room temperature, and the resulting white precipitate was recovered.

Synthesis of Sb^{3+}-doped lithium disilicate ($x = 0.005$, 0.0075, and 0.01)

Appropriate molar amounts of $LiNO_3$ (13.9, 9.9, or 7.92 mmol), $SiO_2.H_2O$ (41.8, 29.81, or 23.92 mmol, respectively), and Sb_2O_3 (0.035, 0.0377, or 0.0549 mmol, respectively) were dissolved in 60 mL of hot NaOH solution (1.40, 0.99, or 0.80 M, respectively) under magnetic stirring at 80°C. The resultant solution was transferred into a 100-mL Teflon-lined stainless steel autoclave. The autoclave was sealed and maintained at 180°C for 48 h then allowed to cool naturally to room temperature, and the resulting white precipitate was recovered.

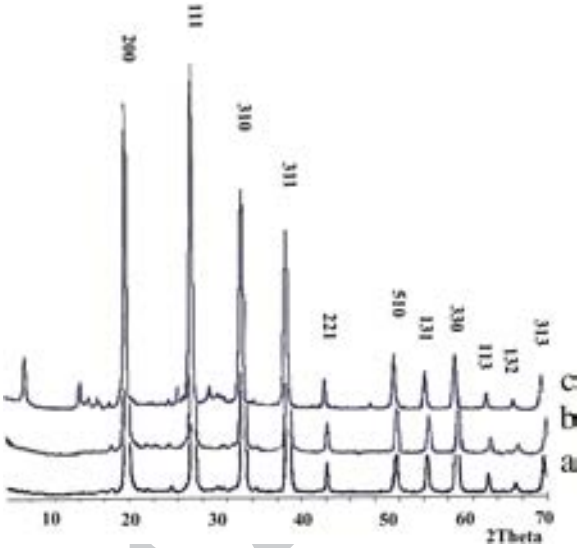

Figure 1 PXRD patterns of the synthesized $Li_{2-2x}Sb_{2x}SiO_3$ nanoparticles, where a is $x = 1$; b is $x = 1.25$; and c is $x = 1.5$ mole%.

Results and discussion

Powder X-ray diffraction analysis

The crystal phases of the synthesized samples were examined by powder X-ray diffraction technique. Figures 1 and 2 show the powder X-ray diffraction (PXRD) patterns of the Sb^{3+}-doped lithium metasilicate and lithium disilicate, respectively. Also, the measured PXRD data for hydrothermally synthesized undoped lithium metasilicate and lithium

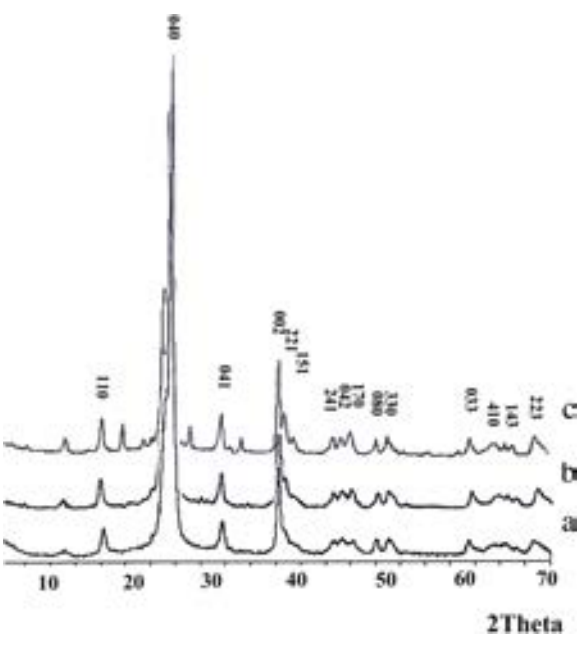

Figure 2 PXRD patterns of the synthesized $Li_{2-2x}Sb_{2x}Si_2O_5$ nanoparticles, where a is $x = 0.5$; b is $x = 0.75$; and c is $x = 1$ mole%.

Table 1 Crystallographic data of the hydrothermally synthesized Li_2SiO_3 nanomaterials obtained after 96 h at 180°C

2θ	Intensity	h	k	l
18.881	82	2	0	0
26.979	100	1	1	1
33.05	57	3	1	0
33.176	28	0	2	0
38.419	22	3	1	1
38.608	47	0	0	2
43.23	7	2	2	1
43.317	5	2	0	2
51.467	4	5	1	0
51.711	10	3	1	2
51.793	13	0	2	2
55.448	9	4	2	1
55.579	8	1	3	1
58.955	10	6	0	0
59.183	18	3	3	0
62.998	6	1	1	3
66.219	2	4	2	2
66.335	2	1	3	2
69.343	2	6	2	0
69.732	11	3	1	3
72.715	8	6	0	2
72.917	13	3	3	2
75.793	4	7	1	1
76.129	3	2	4	1
82.286	3	6	2	2
82.526	4	4	2	3
85.511	4	4	4	1
97.986	2	6	2	3
98.258	2	0	4	3
101.044	2	7	1	3
111.023	2	4	4	3
121.852	2	3	1	5

disilicate nanoparticles are summarized in Tables 1 and 2 respectively. The measured powder XRD data are in good agreement with those of standard pure lithium metasilicate (JCPDS 29-0829) and lithium disilicate (JCPDS 15-0637), and the obtained stable phases are isostructural with Li_2SiO_3 (space group $Cmc2_1$) [32-41] and $Li_2Si_2O_5$ (space group Ccc2) [42-44]. Moreover, the intense sharp diffraction patterns suggest that the as-synthesized products are well crystallized. The doping limitations are 0-0.75 and 0-1.25 mole% of Sb^{3+} for lithium metasilicate and lithium disilicate, respectively. However, for excess mole% concentration of the dopant agent in the reaction mixture, the impurity peaks were observed in the XRD patterns. The diffraction lines at $2\theta \approx 13°$, 26° and 49° are assigned by their peak positions to the excess Sb_2O_3 [35]. As shown in Figures 1 and 2, the formation of the other phases of lithium silicates and raw materials was already detected for higher mole percentage concentration of the dopant agent in the reaction mixture [41,42].

Compared to those of the nanoparticles of pure lithium silicates, the diffraction lines in the powder XRD patterns of the nanoparticles of Sb^{3+}-doped lithium silicates shift to lower 2θ values ($\Delta 2\theta = 26.99$ (pure) – 26.81 (doped) = 0.15° and $\Delta d = 3.322$ Å (doped) – 3.304 Å (pure) = 0.018 Å for Sb^{3+}-doped lithium metasilicate; and $\Delta 2\theta = 24.78$ (pure) – 24.68 (doped) = 0.1°, $\Delta d = 3.603$ Å (doped) 3.589 Å (pure) = 0.014 Å for Sb^{3+}-doped lithium disilicate are calculated via Bragg's law ($n\lambda = 2d_{hkl} \sin \theta$)). Since the ionic radius of the Sb^{3+} (0.76 Å [45]) is closer to the ionic radius of Li^+ (0.59 Å [45]) rather than the Si^{4+} (0.26 Å [45]), in the Sb^{3+}-doped lithium metasilicate

Table 2 Crystallographic data of the hydrothermally synthesized $Li_2Si_2O_5$ nanomaterials obtained after 120 h at 180°C

2θ	Intensity	h	k	l
12.097	12	0	2	0
16.371	6	1	1	0
22.093	2	0	2	1
23.706	45	1	3	0
24.298	100	0	4	0
24.639	30	1	1	1
30.697	2	0	4	1
37.602	4	0	0	2
38.266	4	2	2	1
39.221	4	1	5	1
44.049	2	2	4	1
45.018	2	0	4	2
46.131	30	1	7	0
49.294	2	2	0	2
49.696	2	0	8	0
50.492	2	3	3	0
60.324	2	1	1	3
60.85	2	0	3	3
63.056	2	1	3	3
63.295	16	0	4	3
64.573	2	4	1	0
65.542	4	1	4	3
68.08	2	2	2	3
76.007	6	0	10	2
77.995	2	4	2	2

and lithium disilicate, it may be expected that the dopant ion will replace with Li^+ ions. The larger radius of the dopant ion, as compared to the Li^+, may cause an expansion of the lattice parameter in the Sb^{3+}-doped lithium silicate nanomaterials. Since both ionic radii and charges are not the same for the dopant and Li^+ ions, it is also possible that the dopant ion takes an interstitial position in lattice rather than replaces any Li^+ ions, where additional patterns will be observed in XRD pattern [26]. However, here, the doped samples show similar powder XRD patterns without any residual or impurity phase formation. The powder XRD patterns of the doped samples suggest the fact that the dopant ions are indeed going to lattice positions rather than to interstitial positions. Moreover, when replacing Li^+ ions, the dopant ions are bound to create some oxygen-related defect centers or Li^+ vacancies for charge compensation. Therefore, it is believed that the dopant ions will be in a structurally disordered environment.

Morphology analysis

The scanning electron microscopy (SEM) images of the synthesized Li_2SiO_3 nanomaterials are given in Figure 3. After 48 h, nonuniform sheet like nanoparticles of Li_2SiO_3 are obtained (Figure 3a). The thickness, widths, and lengths of the resultant sheets are approximately 100 nm, 600 nm, and 2 μm respectively. With increasing the reaction time to 72 h, the morphology of the obtained materials has been changed to the very compact sheets with heterogeneous morphology (Figure 3b). This is while, with the reaction time of 96 h, uniform flower like nanoparticles are obtained (Figure 3c).

Figure 4 represents the SEM images of the synthesized $Li_2Si_2O_5$ nanomaterials. After 48 h, the morphology of the obtained material is sponge-like, consisting of sheet-like and flower-like nanoparticles (Figure 4a). With the increasing the reaction time to 72, 96, and 120 h, the morphology of the obtained materials has been changed to the rectangular sheets and high homogeny in the size is achieved. Using field emission scanning electron microscopy, the microstructure analysis of as-synthesized samples was investigated.

SEM images of the synthesized Sb^{3+}-doped lithium metasilicates ($Li_{1.98}Sb_{0.02}SiO_3$) and ($Li_{1.975}Sb_{0.025}SiO_3$) are given in Figures 5 and 6 respectively. In Figure 5a, with low magnification, it is revealed that the sample

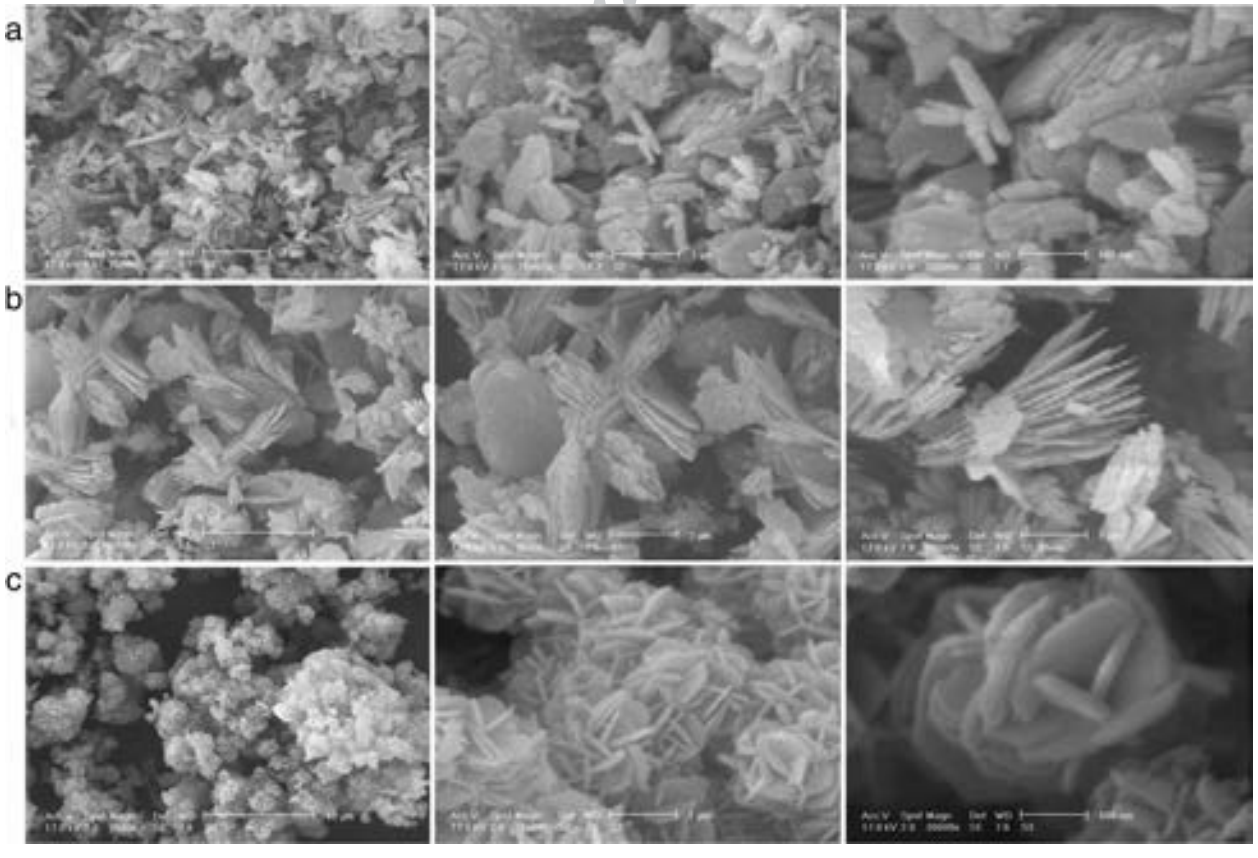

Figure 3 SEM images of the hydrothermally synthesized Li_2SiO_3 nanomaterials obtained after (a) 48, (b) 72, and (c) 96 h at 180°C.

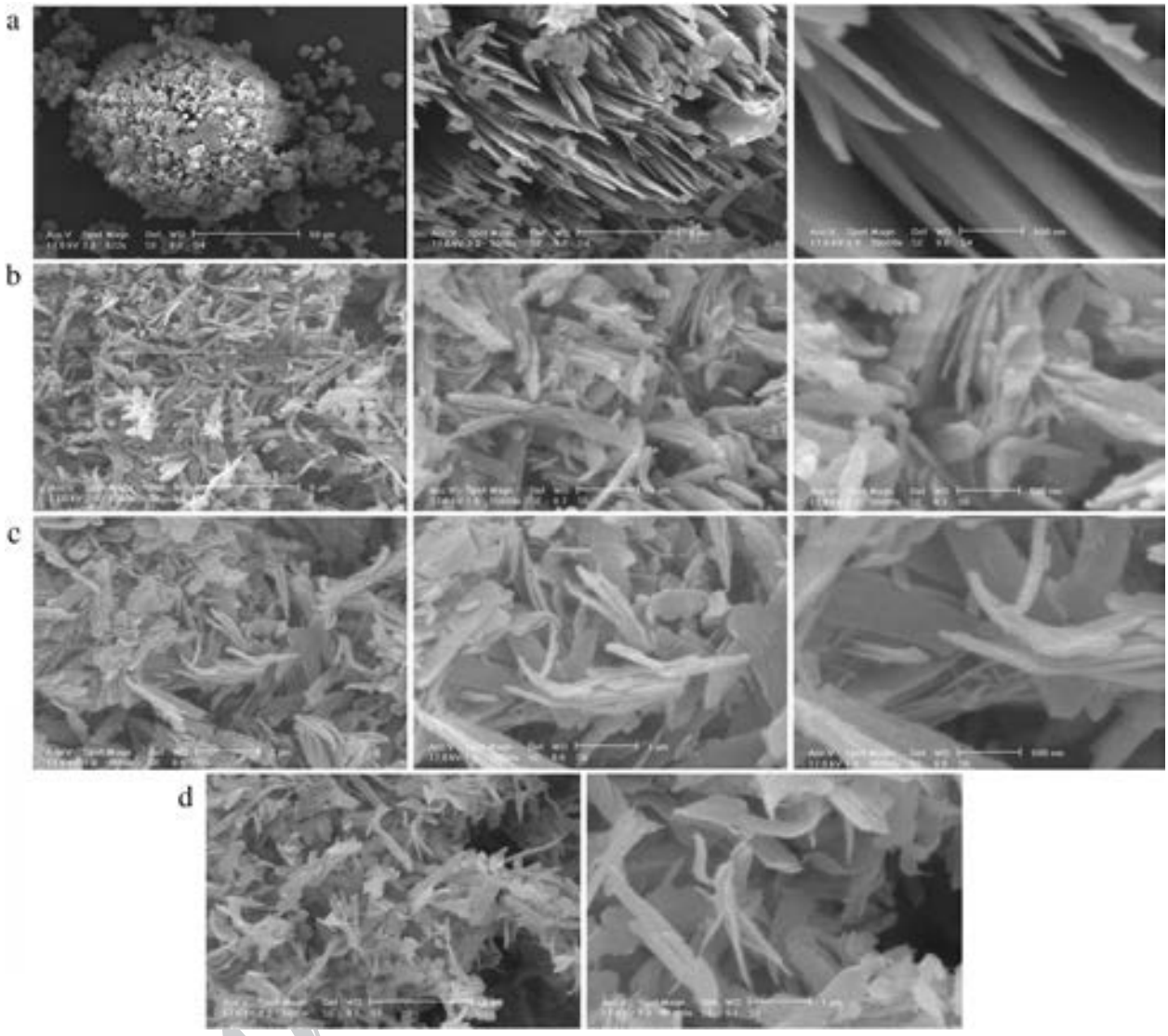

Figure 4 SEM images of the hydrothermally synthesized $Li_2Si_2O_5$ nanomaterials obtained after (a) 48, (b) 72, (c) 96, and (d) 120 h at 180°C.

is composed of two dimensional continuous networks of nanosheet structures. With high magnification in Figure 5b,c, it is clear that the length of the sheets are about 1 μm and the thickness of the sheets is about 100 nm. With high magnification, as shown in Figures 6b,c, there are two types of flower-like structures (showing nonuniformity of the morphology). Low magnification in Figure 6a,b,c shows that the size of each flower is about 3-5 μm and the thickness of the sheets is about 100 nm.

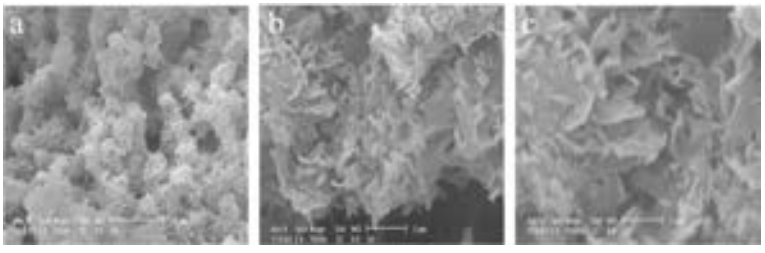

Figure 5 SEM images of the synthesized $Li_{1.98}Sb_{0.02}SiO_3$ nanoparticles.

Figures 7 and 8 show the SEM images of the synthesized Sb^{3+}-doped lithium disilicate ($Li_{1.99}Sb_{0.01}Si_2O_5$) and ($Li_{1.985}Sb_{0.015}Si_2O_5$) respectively. Low magnification in Figure 7a shows that the sample is composed of a large quantity of individual plates. High magnification images in Figure 7b,c shows that the plates cut each other. The length of each plate is about 300-350 nm, and the thickness is 80-100 nm. The plates have regular multigonal shapes that are arisen from a substrate.

Figure 8a shows that with increasing the concentration of Sb^{3+} from 0.5 to 0.75 mole%, the morphology of the samples change from nanoplates to nanoflower structures. The synthesized products are composed of a large quantity of individual nanobelts that form highly uniform 3-D flower-like structures. Each nanobelt has a width of about 500 nm and a length of about 2 μm. It seems that numerous nanodot particles cover all over the surface of each nanobelt.

Optical properties

The optical properties of the as-synthesized materials were measured at room temperature. Figure 9 shows photoluminescence spectra of the synthesized Sb^{3+}-doped lithium metasilicate nanoflowers ($\lambda_{ex} = 232$ nm). It is well known that the emission peak positions remain almost unchanged under different excitation wavelengths, showing that it is an intrinsic property of the compound [44]. Under excitation with light at 232 nm, as shown in Figure 9, the main emission peaks are located at 310 and 362 nm with a shoulder at 425 nm. The peak that

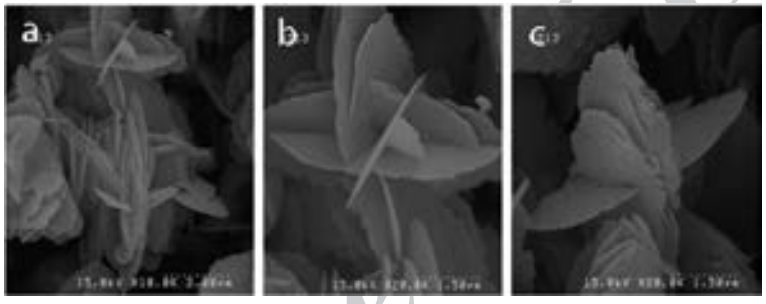

Figure 6 SEM images of the synthesized $Li_{1.975}Sb_{0.025}SiO_3$ nanoparticles.

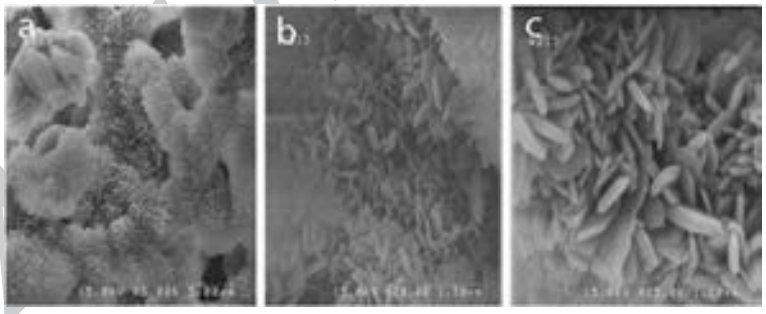

Figure 7 SEM images of the synthesized $Li_{1.99}Sb_{0.01}Si_2O_5$ nanoparticles.

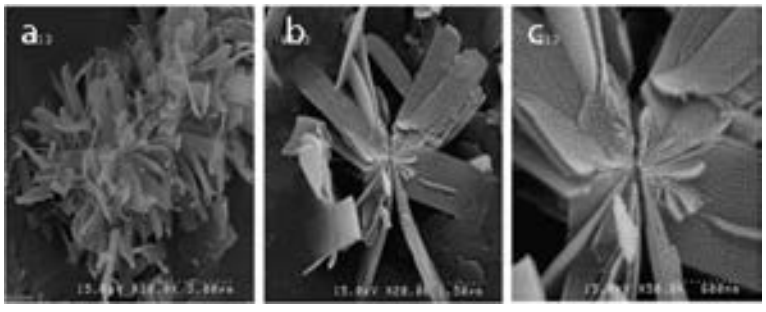

Figure 8 SEM images of the synthesized $Li_{1.985}Sb_{0.015}Si_2O_5$ nanoparticles.

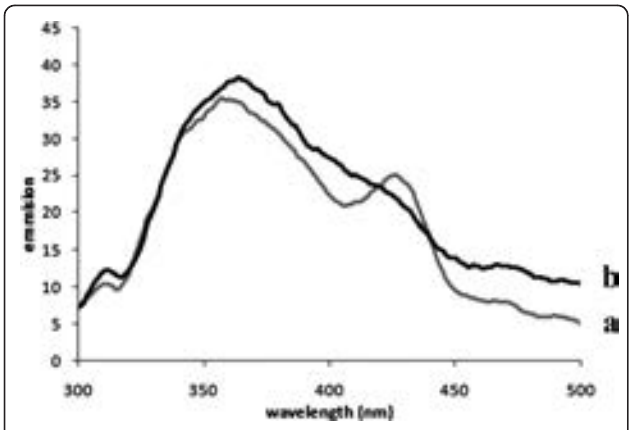

Figure 9 Photoluminescence spectra of the synthesized $Li_{2-2x}Sb_{2x}SiO_3$ nanoflowers ($\lambda_{ex} = 232$ nm), where a is $x = 1$ and b is $x = 1.25$ mole%.

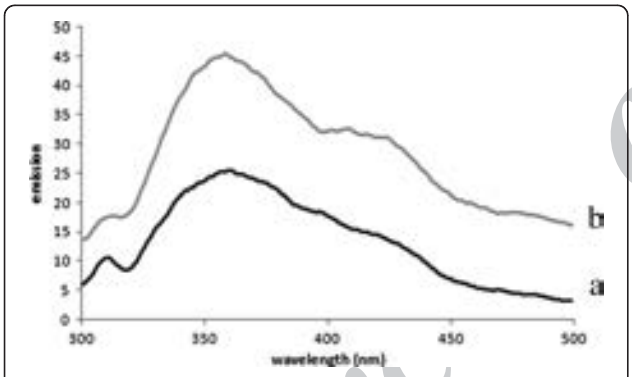

Figure 10 Photoluminescence spectra of the synthesized $Li_{2-2x}Sb_{2x}Si_2O_5$ nanoflowers ($\lambda_{ex} = 227$ nm), where a is $x = 0.5$ and b is $x = 0.75$ mole%.

appeared at 310 nm is assigned to the band edge emission. Also, the broad band with maxima at 362 nm is assigned to the trap state emission of the nanocrystals. With increasing dopant concentration, the intensity of the shoulder at 425 nm also increases. Considering that the energy gap of bulk lithium silicates is above 3.3 eV, the purple-blue photoluminescence at 425 nm (approximately 2.92 eV) is probably due to a triplet to ground state transition of a neutral oxygen vacancy defect, as suggested by *ab initio* molecular orbital calculations for many other well-studied metal oxides [46,47]. The defects create some dangling bands. Therefore, the energy levels between conduction and valence bands (trap states) would contribute in the band structure, which result in a broad band at visible range.

The photoluminescence spectra of the synthesized Sb^{3+}-doped lithium disilicate nanoflowers ($\lambda_{ex} = 227$ nm) is given in Figure 10. Compared to the described antimony-doped lithium metasilicate nanomaterials, the band edge emission of the synthesized Sb^{3+}-doped lithium disilicate nanomaterials occurred at 310 nm upon excitation at 227 nm. Also, the trap state emission of the compound is observed as a weak band at 360 nm under this excitation wavelength. Moreover, compared to the synthesized antimony-doped lithium metasilicate nanomaterials, the emission band which is attributed to the oxygen-related defects in Sb^{3+}-doped lithium disilicate nanoflowers (appeared as a shoulder at 425 nm) shows a decreasing intensity with the increasing dopant concentration. Electronic absorption spectra of the as-synthesized Sb^{3+}-doped Li_2SiO_3 and $Li_2Si_2O_5$ nanomaterials have been given in Figure 11a,b. With increasing the dopant concentration in the structure of both of the synthesized Sb^{3+}-doped lithium silicates, the band gap slightly shifts to lower energies. A band gap of 4.17 eV for $Li_{1.98}Sb_{0.02}SiO_3$ and 4.13 eV for $Li_{1.975}Sb_{0.025}SiO_3$ is calculated from the absorption spectroscopy. Also, a band gap of 4.49 eV and 4.46 eV, respectively, was measured for $Li_{1.99}Sb_{0.01}Si_2O_5$ and $Li_{1.985}Sb_{0.015}Si_2O_5$ from the electronic absorption spectroscopy.

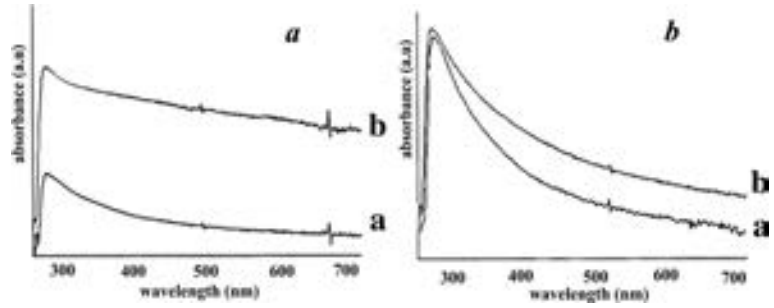

Figure 11 The electronic absorption spectra of the synthesized $Li_{2-2x}Sb_{2x}SiO_3$ nanomaterials, (a) where a is $x = 1$ and b is $x = 1.25$ mole % and (b) where a is $x = 0.5$ and b is $x = 0.75$ mole%.

Conclusions

In summary, nanolayers and nanoflowers of Sb^{3+}-doped lithium metasilicate and lithium disilicate were synthesized successfully by employing a simple hydrothermal method. We found that the dopant concentration affects the morphology and crystal phase of the final product. As shown by SEM images, with increasing the dopant concentration, layered and flake-like nanocrystals change to flower-like nanomaterials. We found that compared to those of the nanoparticles of pure lithium silicates, the diffraction lines in the powder XRD patterns of the nanoparticles of Sb^{3+}-doped lithium silicates shift to lower 2θ values. The shift in the diffraction lines might be attributed to the larger radius of the dopant ion, compared to the ionic radius of the Li^+, which may cause an expansion of the lattice parameters in the Sb^{3+}-doped lithium silicate nanomaterials. The synthesized nanomaterials exhibited emerging photoluminescence and electronic absorption optical properties in the UV-visible region, which show dependence on the dopant amounts in the structure. These materials are expected to have a potential application in light-emitting devices and as catalysts.

Competing interests

The authors declare that they have no competing interest.

Authors' contributions

All authors participated in the experiments, read and approved the final manuscript.

Authors' information

SK got his B.S. degree from the University of Birjand in the field of applied chemistry in 2007. He got his M. Sc degree from the University of Tabriz in the field of inorganic chemistry in August 2010. AA got his B.S. and M. Sc. degree from the University of Tabriz, Iran in the field of chemistry in 1972 and 1974, respectively. She got her Ph. D degree from the University of Paris, France in the field of inorganic chemistry in 1978. He is now a professor in inorganic chemistry at University of Tabriz, Iran. MD got her B.S. and M. Sc. degree from the University of Tabriz, Iran in the field of chemistry and inorganic chemistry in 2004 and 2006, respectively. She got her Ph. D degree from the University of Tabriz, Iran in the field of inorganic-solid state chemistry in 2010. She is now post doctorate student and associate professor in the research group of Prof. Dr. Rostami at School of Engineering-Emerging Technologies, University of Tabriz, Iran. AB got his B.S. and M. Sc. degree from the University of Urmia, Iran and from the University of Tabriz in the field of chemistry and inorganic chemistry in 2004 and 2006, respectively. She got her Ph. D degree from University of Tabriz, Iran in the field of inorganic chemistry in 2010.

Acknowledgment

The authors express their sincere thanks to the authorities of University of Tabriz for financing the project.

Author details

[1]Department of Inorganic Chemistry, Faculty of Chemistry, University of Tabriz, Tabriz, Iran. [2]Laboratory of Photonics and Nano Crystals, School of Engineering-Emerging Technologies, University of Tabriz, Tabriz, Iran.

Received: 21 April 2012 Accepted: 3 September 2012
Published: 19 September 2012

References

1. Kudo, H, Okuno, K, Ohira, S: Tritium release behavior of ceramic breeder candidates for fusion reactors. J. Nucl. Mater. **155**, 524 (1988)
2. Wen, G, Zheng, X, Song, L: Effects of P_2O_5 and sintering temperature on microstructure and mechanical properties of lithium disilicate glass-ceramics. Acta. Mater. **55**, 3583 (2007)
3. Yamaguchi, T, Nair, BN, Nakagawa, K: Membranes for high temperature CO_2 separation: part II - lithium silicate based membranes. J. Membr. Sci. **294**, 16 (2007)
4. Essaki, K, Kato, M, Nakagawa, K: CO_2 removal at high temperature using packed bed of lithium silicate pellets. J. Ceram. Soc. Japan **114**, 739 (2006)
5. Pfeiffer, H, Bosch, P, Bulbulian, S: Synthesis of lithium silicates. J. Nucl. Mater. **257**, 309 (1998)
6. Mosqueda, HA, Vazquez, C, Bosch, P, Pfeiffer, H: Chemical sorption of carbon dioxide (CO_2) on lithium oxide (Li_2O). Chem. Mater. **18**, 2307 (2006)
7. Ilyushin, GD: Phase relations in the LiOH-TiO_2-SiO_2-H_2O system at 500°C and 0.1 GPa. J. Inorg. Mater. **9**, 927 (2002)
8. Kumar, GB, Buddhudu, S: Synthesis and emission analysis of RE^{3+} (Eu^{3+} or Dy^{3+}):Li_2TiO_3 ceramics. Ceram. Int. **35**, 521 (2009)
9. Romanowski, WR, Sokolska, I, Dsik, GD, Golab, S: Investigation of $LiXO_3$ (X = Nb, Ta) crystals doped with luminescent ions: recent results. J. Alloys Compd. **300301**, 152 (2000)
10. Hreniak, D, Speghini, A, Bettinelli, M, Strek, W: Spectroscopic investigations of nanostructured LiNbO3 doped with Eu^{3+}. J. Lumin. **119–120**, 219 (2006)
11. Yang, X, Ning, G, Li, X, Lin, Y: Synthesis and luminescence properties of a novel Eu^{3+}-doped γ-$LiAlO_2$ phosphor. Mater. Lett. **61**, 4694 (2007)
12. Ignatovych, M, Holovey, V, Vidczy, T, Baranyai, P: Spectral study on manganese- and silver-doped lithium tetraborate phosphors. Radiat. Phys. Chem. **76**, 1527 (2007)
13. Ganesan, M: Li_{1-x} Sm_{1+x} SiO_4 as solid electrolyte for high temperature solid-state lithium batteries. Ionics **13**, 379 (2007)
14. Ganesan, M, Dhananjeyan, MVT, Sarangapani, KB, Renganathan, NG: Lithium ion conduction in sol-gel derived lithium samarium silicate solid electrolyte. J. Alloy Comp. **450**, 452 (2008)
15. Ganesan, M: Synthesis and characterization of lithium holmium silicate solid electrolyte for high temperature lithium batteries. J Appl. Electrochem. **39**, 947 (2009)
16. Ganesan, M: A new promising high temperature lithium battery solid electrolyte. Electrochem. Commun. **9**, 1980 (2007)
17. Takeda, N, Itagaki, Y, Sadaoka, Y: Ionic conductivity of $Li_xLa_{10-x}(SiO_4)_6O_{3-x}$ sinters. J. Cer. Soc. Japan **116**, 803 (2008)
18. Naik, YP, Mohapatra, M, Dahale, ND, Seshagiri, TK, Natarajan, V, Godbole, SV: Synthesis and luminescence investigation of RE^{3+} (Eu^{3+}, Tb^{3+} and Ce^{3+})-doped lithium silicate (Li_2SiO_3). J. Lumin. **129**, 1225 (2009)
19. Deng, D, Xu, S, Ju, H, Zhao, S, Wang, H, Li, C: Broadband near-infrared emission from Cr4+- doped transparent glass-ceramics based on lithium silicate. Chem. Phys. Lett. **486**, 126 (2010)
20. Nakazawa, T, Yokoyama, K, Noda, K: *Ab initio* MO study on hydrogen release from surface of lithium silicate. J. Nucl. Mater. **258–263**, 571 (1998)
21. Victoria, L, Trejo, M, Fregoso-Israel, E, Pfeiffer, H: Textural, structural, and CO_2 chemisorption effects produced on the lithium orthosilicate by its doping with sodium ($Li_{4-x}Na_xSiO_4$). Chem. Mater. **20**, 7171 (2008)
22. Rodriguez, VD, Rodriguez-Mendoza, UR, Martin, IR, Lavin, V, Nunez, P: Site distribution in Cr^{3+} and Cr^{3+}- Tm^{3+}-doped alkaline silicate glasses. J. Lumin. **72–74**, 446 (1997)
23. Elbatal, HA, Mandouh, Z, Zayed, H, Marzouk, SY, Elkomy, G, Hosny, A: Gamma ray interactions with undoped and CuO-doped lithium disilicate glasses. Physica B: Cond. Mat. **405**, 4755 (2010)
24. Abd, E, All, S, Ezz-Eldin, FM: Beam interactions with materials and atoms. Nucl. Instrum. Methods Phys. Res., B **268**, 49 (2010)
25. Yang, W, Cai-mei, F, Bo, H, Hai, LZ, Pin, SY: Photoelectrocatalytic activity of two antimony doped SnO_2 films for oxidation of phenol pollutants. Trans. Nonferrous Met. Soc. China **19**, 778 (2009)
26. Sen, RD, Min, BZ, Li, H, Jie, S, Li, CX, Ling, YX, Jian, ZZ: The effect of dopant Sb on the superhydrophilicity and the microstructure of the nanoscale TiO_2 thin film. Acta Phys. Chim. Sin. **20**, 414 (2004)
27. Mandalapu, LJ, Yang, Z, Xiu, FX, Zhao, DT, Liu, JL: Homojunction photodiodes based on Sb-doped *p*-type ZnO for ultraviolet detection. Appl. Phys. Lett. **88**, 092103 (2006)
28. Hu, Y, Hou, SH: Preparation and characterization of Sb-doped SnO_2 thin films from colloidal precursors. Mater. Chem. Phys. **86**, 21 (2004)
29. Lee, SY, Park, B: Structural, electrical and optical characteristics of SnO_2:Sb thin films by ultrasonic spray pyrolysis. Thin Solid Films **510**, 154 (2006)

30. Lupan, O, Chow, L, Ono, LK, Cuenya, BR, Chai, G, Khallaf, H, Park, S, Schulte, A: Synthesis and characterization of Ag- or Sb-doped ZnO nanorods by a facile hydrothermal route. J. Phys. Chem. **114**, 12401 (2010)
31. Mandalapu, LJ, Xiu, FX, Yang, Z, Liu, JL: Al/Ti contacts to Sb-doped *p*-type ZnO. J. Appl. Phys. **102**, 023716 (2007)
32. Gutiérrez, GM, Cruz, D, Pfeiffer, H, Bulbulian, S: Low temperature synthesis of Li2SiO3: effect on its morphological and textural properties. Res. Lett. Mater. Sci. (2008) doi: 10.1155/2008/908654
33. Zhang, B, Easteal, AJ: Effect of HNO_3 on crystalline phase evolution in lithium silicate powders prepared by sol-gel processes. J. Mater. Sci. **43**, 5139 (2008)
34. Fuss, T, Moguš-Milanković, A, Ray, CS, Lesher, CE, Youngman, R, Day, DE: *In-situ* crystallization of lithium disilicate glass: effect of pressure on crystal growth rate. J. Non-Cryst. Sol. **352**, 4101 (2006)
35. Soares, PC, Zanotto, ED, Fokin, VM, Jain, H: TEM and XRD study of early crystallization of lithium disilicate glasses. J. Non-Cryst. Sol. **331**, 217 (2003)
36. Zheng, X, Wen, G, Song, L, Huang, X: Effects of P_2O_5 and heat treatment on crystallization and microstructure in lithium disilicate glass ceramics. Acta Mater. **56**, 549 (2008)
37. Mahmoud, MM: Crystallization of lithium disilicate glass using variable frequency microwave processing., Blacksburg, Virginia (2007)
38. Ge, S, Wang, Q, Li, J, Shao, Q, Wang, X: Controllable synthesis and formation mechanism of bow-tie-like Sb_2O_3 nanostructures via a surfactant-free solvothermal route. J. All. Comp. **494**, 169 (2010)
39. Deng, Z, Chen, D, Tang, F, Ren, J, Muscat, AJ: Synthesis and purple-blue emission of antimony trioxide single-crystalline nanobelts with elliptical cross section. Nano. Res. **2**, 151 (2009)
40. Grund, CS, Hanusch, K, Breunig, JH, Wolf, HU: Antimony and antimony compounds. In: Ullmann's Encyclopedia of Industrial Chemistry. Weinheim, Wiley-VCH (2006)
41. De Jong, BHW, Beerkins, RGC, van Nijnatten, PA, Bourhis, EL: Glass. In: Ullmann's Encyclopedia of Industrial Chemistry. Weinheim, Wiley-VCH (2005)
42. Peiniger, M, Piel, H: A superconducting Nb_3Sn coated multicell accelerating cavity. J. Nucl. Sci. **32**, 3610 (1985)
43. Moura, S, Hernane, R: Melting and purification of niobium. In: Single Crystal - Large Grain Niobium Technology: AIP Conference Proceedings. American Institution of Physics, Melville **927**, 165 (2007)
44. Ye, C: Low temperature growth and photoluminescence of well-aligned zinc oxide nanowires. Chem. Phys. Lett. **363**, 134 (2002)
45. Lide, DR: CRC Handbook of Chemistry and Physics. Boca Raton: Taylor and Francis, 87th ed (2006)
46. Hsu, J, Tallant, DR, Simpson, RL, Missert, NA, Copel, RG: Luminescent properties of solution-grown ZnO nanorods. Appl. Phys. Lett. **88**, 252103 (2006)
47. Her, YC, Wu, JY, Lin, YR, Tsai, SY: Low-temperature growth and blue luminescence of SnO_2 nanoblades. Appl. Phys. Lett. **89**, 043115 (2006)

doi:10.1186/2228-5326-2-20
Cite this article as: Alemi *et al.*: **Hydrothermal synthesis, characterization, and investigation of optical properties of Sb^{3+}-doped lithium silicates nanoparticles.** *International Nano Letters* 2012 **2**:20.